Bulgarian Chemical Communications, Volume 47, Special Issue D (pp. 49 – 55) 2015

Determination of methane hydrate interfacial tension from measurement of induction time in methane hydrate crystallization

Alireza Azimi, Masoomeh Mirzaei , Seyed Mostafa Tabatabaee Ghomshe

Department of Chemical Engineering, Mahshahr Branch, Islamic Azad University, Mahshahr, Iran.

Submitted

Abstract: In this work the interfacial tension between methane hydrate and water at various temperatures, pressures and solution concentrations is determined. The Induction time in methane hydrate crystallization has been evaluated in a batch system and correlation of the induction time with the solution supersaturation has been drawn by the Classical Nucleation Theory (CNT). The results have shown that the induction time decreases with increasing solution concentration at any constant temperature while the interfacial tension increases with rising temperature. Experimental values of Hydrate – Water interfacial tension are evaluated 1.22, 1.957 and 4.16 at three temperatures as 273.15, 273.65 and 274.65 K. An empirical correlation has been used and the order of nucleation is thereby obtained to be 1.189.

Key words: Interfacial tension, Methane hydrate, Induction time, Crystallization, Nucleation

INTRODUCTION

Gas hydrates are ice-like compounds that are formed by a mixture of water and light gas molecules such as methane, ethane, CO_2, H_2S, Ar, Kr, Xe, … at low temperatures and high pressures [1-4]. The crystal lattice is made up of water molecules which are strongly hydrogen bonded "host" and gas molecules "guest" that are engaged in cavities formed in the clathrates [5,6]. Gas hydrates are non-stoichiometric crystalline inclusion compounds comprised of approximately 85 mol% water, 15 mol% guest gas, and thermodynamically stable at low temperatures and high pressures [7]. Kinetics models proved that gas hydrate formation in general is a crystallization process including nucleation and growth steps [8-10]. Nucleation is an interfacial phenomenon, so interfacial properties like interfacial tension has a high effect on the rate of hydrate formation [11-13]. In this work the interfacial tension between methane hydrate and water has been determined by measurement of the induction time in methane hydrate crystallization. Induction time of crystallization depends on the temperature and the level of supersaturation [14]. In general, the induction time decreases with increasing supersaturation and rising temperature [15,16].

PROBLEM DESCRIPTION

A relation to evaluate the nucleation rate in supersaturated solutions is derived from classical nucleation theory (CNT) by Mullin [17]:

$$B = B^0 \exp\left(-\frac{\Delta G}{kT}\right) \qquad (1)$$

In Equation (1) ΔG is the change of Gibbs free energy between a small particle of the dissolved substance and the solute in solution including two terms: the surface free energy and the volume free energy.

$$\Delta G_s = 4\pi r^2 \gamma \ , \ \Delta G_v = 4/3\, \pi r^3 g_v \qquad (2)$$

Considering the maximum value of ΔG at the critical nucleus size, Mullin [17] derived Gibbs-Thomson relation to calculate the nucleation rate.

$$B = B^0 \exp\left(-\frac{16\pi\gamma^3 V_m^2}{3(kT)^3 \ln S^2}\right) \qquad (3)$$

Where $S = C/C^*$ is supersaturation, k is Boltzmann constant by value of $k = 1.3805\times10^{-23}\frac{j}{K}$, T is temperature , γ is the interfacial tension and V_m is the molecular volume of methane which is calculated from following equation:

$$V_m = \frac{z\,R\,T}{P\,N_A} \qquad (4)$$

In Equation (4) z is the compressibility factor of methane, $R = 8.314\frac{N..m}{mol.K}$ is the gas constant and N_A is the Avogadro's number.

The induction time is assumed to be inversely proportional to the nucleation rate, $t_{ind} \propto \frac{1}{B}$, which gives Mullin [17] and Ghader [14] :

$$t_{ind} = K \exp\left(\frac{16\pi\gamma^3 V_m^2}{3(kT)^3 (\ln S)^2} \right) \quad (5)$$

$$\ln(t_{ind}) = \ln(K) + \left(\frac{16\pi\gamma^3 V_m^2}{3(kT)^3 (\ln S)^2} \right) \quad (6)$$

Which means that at different temperatures, a plot of $\ln(t_{ind})$ versus $\frac{1}{T^3 (\ln S)^2}$ should yield a straight line with slope m defined as:

$$m = \frac{16\pi\gamma^3 V_m^2}{3k^3} \quad (7)$$

The interfacial tension between the nuclei and solution is therefore:

$$\gamma = k \left(\frac{3m}{16\pi V_m^2} \right)^{\frac{1}{3}} \quad (8)$$

EXPERIMENTAL INVESTIGATION

Material

Required methane with 99.995 mol% purity was prepared by the Technical Gas Services co. and distilled water was applied as pure water.

Apparatus

The pressure cell made of 316 stainless steel has a volume of about 460 ml. For visual observation a glass window has been placed in the hydrate cell and an ultramodern CCD camera with high focus power is used for monitoring gas hydrate formation.

The data from camera is sent to a computer using Honestech TVR software. The stirring rate of vessel is 60 rpm. Cooling of the vessel is supplied by ethanol circulation in the jackets (Figure 1). To monitor and report temperature in different places into the shell of the cell three thermocouples are used with ±0.1K accuracy at 0.1s time intervals. The accuracy and time interval of cell pressure measurement are 0.1 bar and 0.1 s, respectively. Schematic diagram of the experimental apparatus is shown in Figure (1).

Procedure

At first, the cell was washed with deionized water. To ensure that all parts of set up is free of any air; inner parts were evacuated with a vacuum pump. 100 ml of deionized water was entered into the cell at room temperature and atmospheric pressure. To achieve the desired pressure the cell the cell was charged with methane. After the cell was pressurized, the system was cooled. Initial temperature is about 5K below the anticipated hydrate-formation temperature. As temperature and pressure were monitored continuously, initial nucleation was eventually verified through visualization of the cell content. This was further confirmed by the fact that at the instance of hydrate formation, migration of methane to the solid phase leads to the release of the crystallization energy and a drop in methane concentration in water. This in turn causes a more tendency of methane to be absorbed in water from the gas and the release of absorption energy. The overall outcome is a relatively sudden decrease in the vessel pressure and an increase in the temperature. These events can only be observed if the rate of heat transfer to the coolant ethanol is temporarily kept at nearly zero when nucleation is about to take place, which turns the procedure into one which needs lots of delicate control. Results are later analyzed through

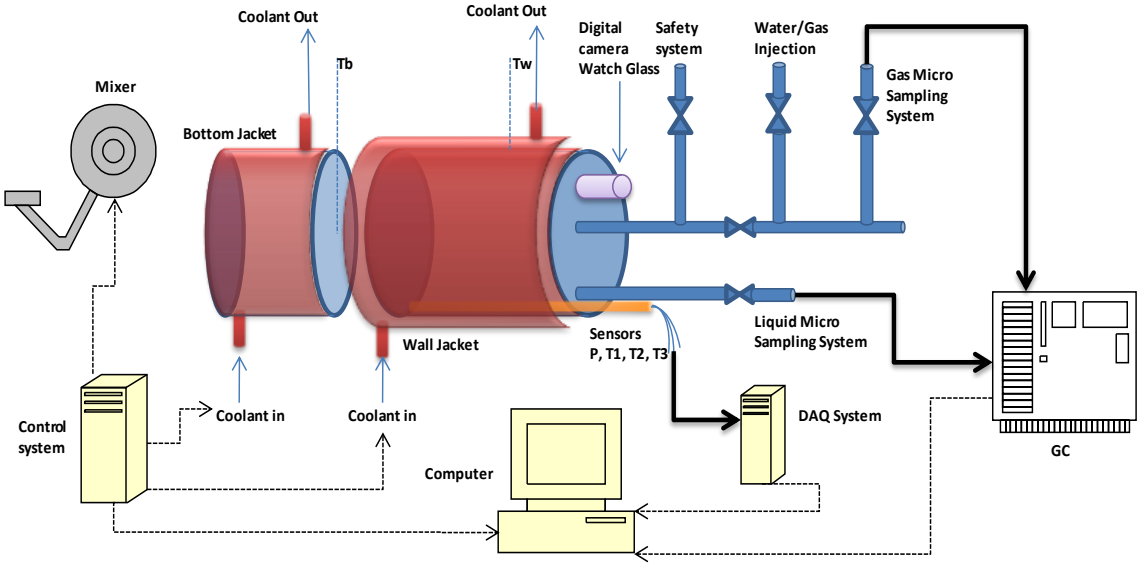

Fig.1. Schematic diagram of experimental apparatus

study of the temperature and pressure profiles and the judged moments of nucleation are compared with results of the visual observations.

RESULTS AND DISCUSSION

Cell temperature and pressure were monitored and measured throughout the experiments. Using these data, the effect of parameters such as supersaturation and temperature on the induction time has been investigated. The cell pressure-temperature profiles during one of the experiments have been drawn in Figure 2. The first section of Figure 2 is shown in Figure 3 in larger scale to help determining the induction time from temperature and pressure profiles with higher accuracy. As seen in Figure 3, at the first stages of the experiment, while cooling the cell, a decline in the pressure is observed which can be attributed to lowering the temperature and gas dissolution in water. These drops in temperature and pressure approach a minimum as the vessel temperature comes close to that of the coolant ethanol. Under this delicately controlled condition, when the methane concentration in water reaches a maximum value and a peak in its concentration and supersaturation in the aqueous media is achieved, the pressure and temperature profiles become flat. This condition will remain unchanged till the eruption of nucleation. The induction time will then be accurately measured by determination of the duration of constant temperature and pressure in this procedure. In each experiment, the instance of nucleation has been determined both by monitoring the end of the flat period in the temperature-pressure profiles from Figure 3 and also by the turbidity observed by the visual apparatus. A comparison of the results is shown in Figure 4.

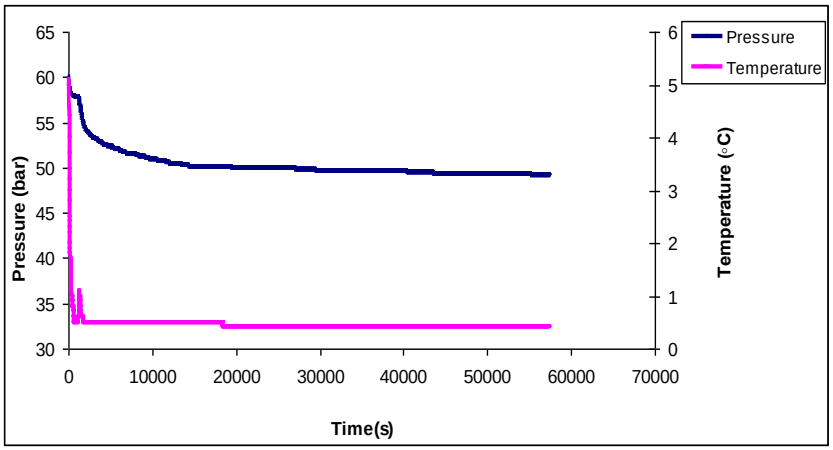

Fig. 2: Cell pressure and temperature profiles for Run (7).

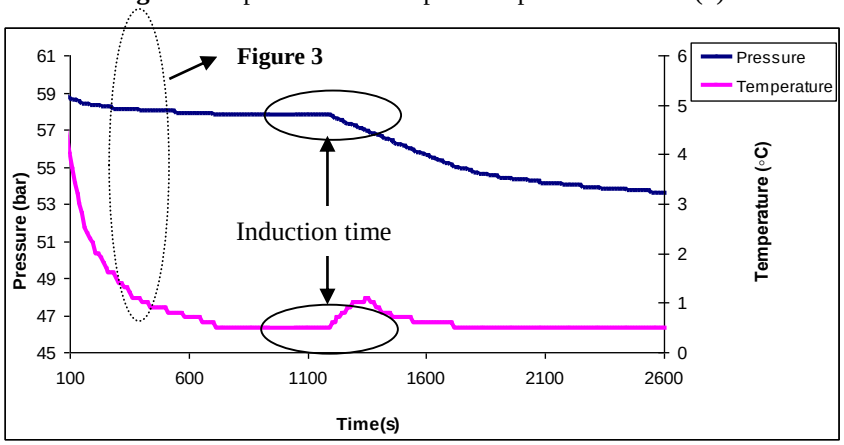

Fig. 3. Induction time determination from the pressure and temperature data for Run (7).

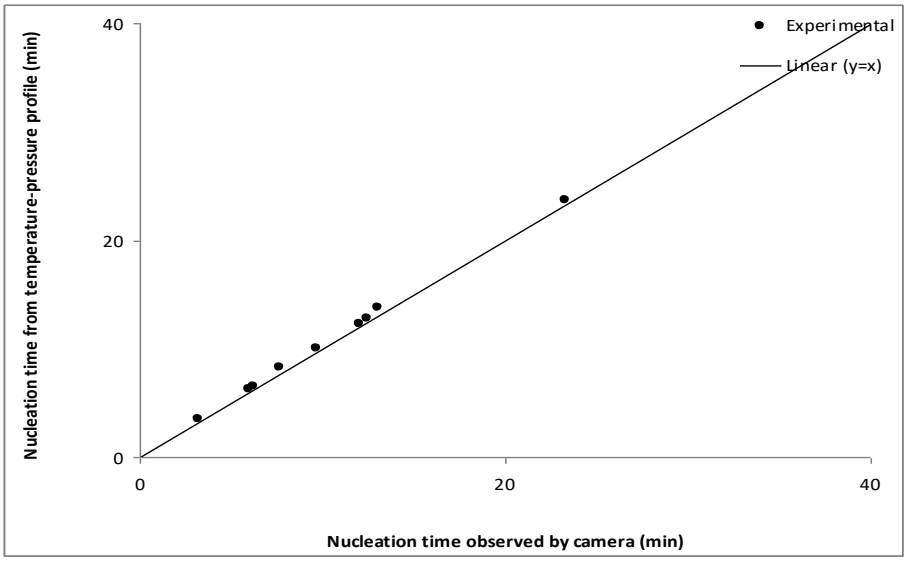

Fig. 4. Comparison of the nucleation time determined by visual observation and pin-pointed from the temperature-pressure profile.

In this figure, the vertical axis is nucleation time determined by temperature-pressure profiles and the axial
axis is the nucleation time observed by camera. By drawing a straight line from the origin with the slope 1, it can be seen that the occurrence of nucleation phenomenon can be determined by both methods equally well.

SUPERSATURATION EFFECT

Solubility of methane hydrate in water has been gathered from literature [18]. Results show that the induction time decreases with increasing supersaturation, satisfying the general trend in Equation (6). In order to compare the experimental induction time results with predictions from the CNT at constant temperature $\ln t_{ind}$ was plotted against $\frac{1}{(\ln S)^2}$. Figure 5 illustrates that a linear relation can be concluded. The values of R^2 of the linear regression are 0.959, 0.967, and 0.960, respectively.

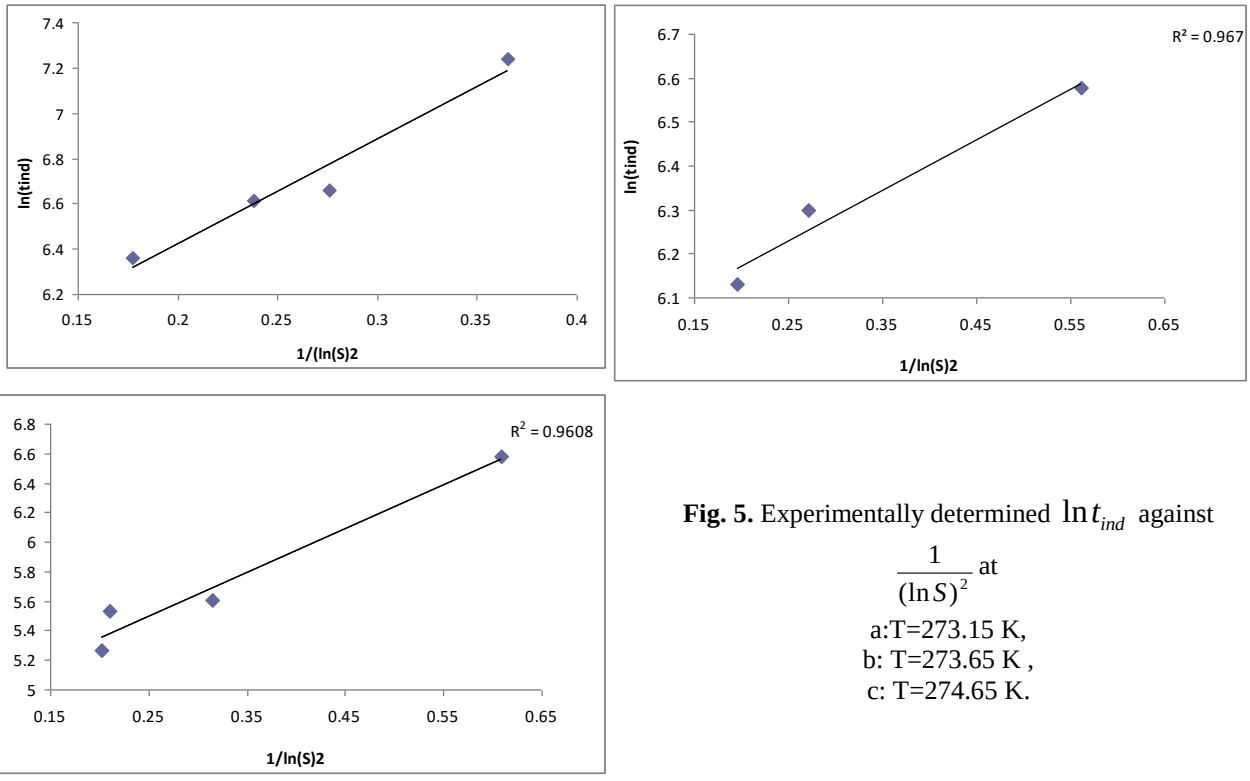

Fig. 5. Experimentally determined $\ln t_{ind}$ against $\frac{1}{(\ln S)^2}$ at
a:T=273.15 K,
b: T=273.65 K ,
c: T=274.65 K.

Determination of the interfacial tension

As Equation (6) shows, the classical nucleation theory (CNT) predicts that at different temperatures a linear relation between $\ln t_{ind}$ and $\frac{1}{T^3(\ln S)^2}$ (with slope m) should exist. All induction time data of methane hydrate at T=273.15 K, T=273.65 K and T=274.65 K are presented in Figure (6) and the prediction of the Classical Nucleation Theory is presented by the slanted line.

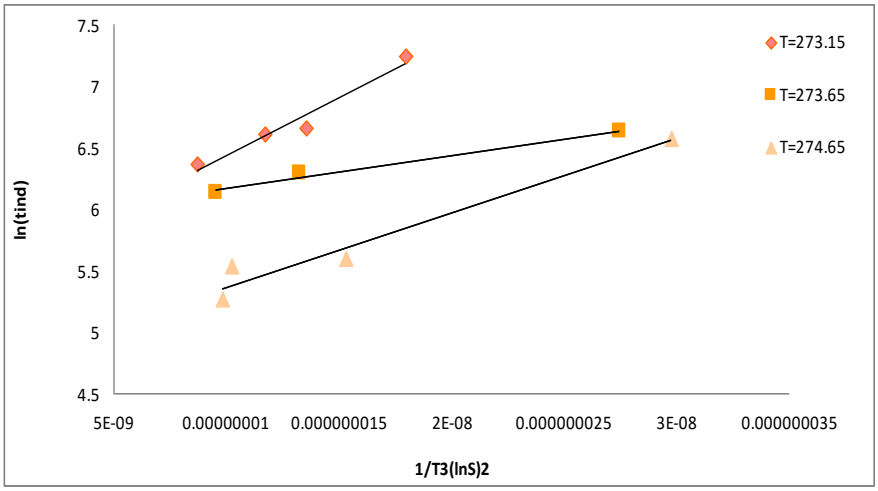

Fig. 6. Measured data of $\ln t_{ind}$ vs. $\frac{1}{T^3(\ln S)^2}$ at different temperatures.

A linear relation is observed. Equation (8) has been used to determine the values of the interfacial tension. The estimated interfacial tension values at different temperatures are shown in Table (1). The results show that Interfacial tension value is rising with temperature increasing. The temperature dependence of the solubility of gas in liquid and the Induction time is the main cause of the interfacial tension variation by temperature.

The findings can be compared with the results given by Equations (9) and (10).

$$\gamma = 0.414k.T\left(C_S.N_A\right)^{\frac{2}{3}}\ln\left(\frac{C_s}{C^*}\right)$$ Mersmann [19] (9)

$$\gamma = k.T.V_m^{-\frac{2}{3}}(0.25)(0.7-\ln x^*),$$ cf. Bennema and Sohnel [20] (10)

In Equation (9) C_S is concentration of methane hydrate in the liquid phase, C^* is the solubility of methane hydrate in water. The experimental values of C^* are estimated 0.059, 0.061 and 0.064 at three temperatures as 273.15, 273.65 and 274.65 K respectively [18]. In equation (10) x^* is the solubility mole fraction of methane hydrate in water is calculated by values of C^*.The results of Equations (9) and (10) are also shown in Table. 1 for comparison. It is found that the values of the interfacial tension obtained in this work compare with predictions by Equation (10) rather more satisfactorily than by Equation (9). It may be attributed to the presence of the term $V_m^{-\frac{2}{3}}$ in both Equations (8) and (10). In Figure (7) the interfacial tension values at different temperatures and levels of supersaturation are shown. It is obvious that changes in supersaturation have little effect on the interfacial tension.

Table 1. Interfacial tension of methane hydrate at different temperatures as estimated by applying experimental results into the CNT and values calculated using Equation (9) and Equation (10).

Temperature (K)	Experimental $\gamma(\frac{mN}{m})$	Equation (9) $\gamma(\frac{mN}{m})$	Equation (10) $\gamma(\frac{mN}{m})$
273.15	1.22	0.011176	9.378
273.65	1.957	0.0134	9.4394
274.65	4.16	0.0149	9.4898

Determination of the order of the nucleation

An empirical correlation is used to correlate the nucleation rate with the level of supersaturation.

$$B = K_b S^n \quad (11)$$

$$t_{ind} = KS^{-n} \quad (12)$$

$$\ln t_{ind} = \ln K - n\ln S \quad (13)$$

Fitting a straight line to the data of $\ln t_{ind}$ vs. $\ln S$ yields the value of the nucleation order.

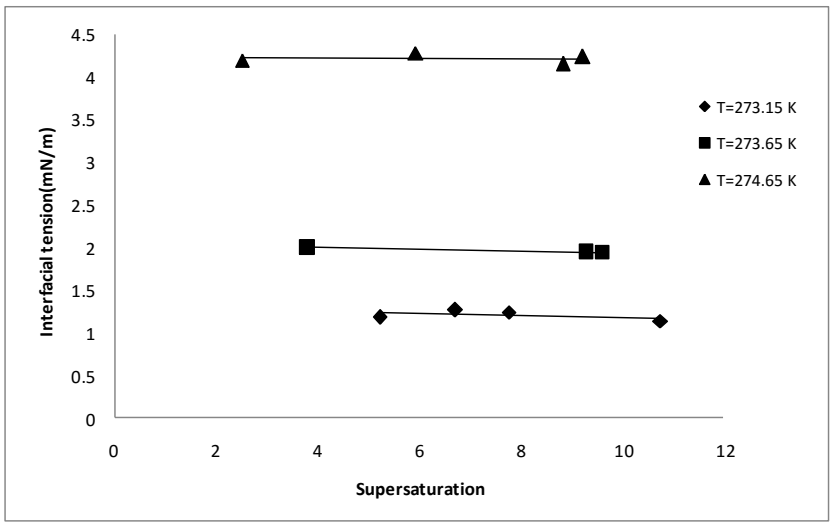

Fig. 7. Interfacial tension values at different temperatures and supersaturation values.

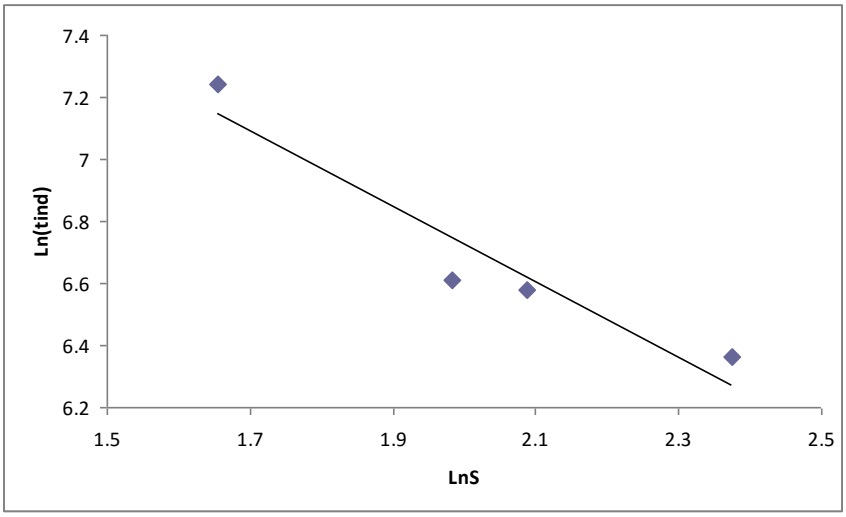

Fig. 8. A plot of Eq. (13) for calculation of the nucleation order at T=273.15 K.

In Figure 8, $\ln t_{ind}$ is plotted against $\ln S$ for calculation of the nucleation order at T = 273.15 K. The values of R^2 of the linear regression are 0.938 and n =1.189.

CONCLUSION

The induction time of methane hydrate crystallization is measured at various temperatures and supersaturation values. The experimental data indicate that the induction time decreased with increasing supersaturation at each constant temperature. The induction time data have satisfactorily been fitted into the Classical Nucleation Theory and the interfacial tension between methane hydrate and the solution has thereby been determined at 3 temperatures. The interfacial tension has been found to increase with rising temperature but changes in supersaturation has little effect. The nucleation order has also been determined by applying the results into the power law correlation for nucleation.

Acknowledgement: *This paper was extracted from a research project entitled "Modeling of methane hydrate crystallization using particle size distribution". Financial assistance from the Islamic Azad University - Mahshahr Branch is gratefully acknowledged.*

Nomenclature

B, *Number/m³.s* - nucleation rate
B^0, *Number/m³.s* - pre-exponential value
C , *mol/L* - concentration
C_S, *mol/L* - concentration of hydrate in the liquid phase
C*, *mol/L* - saturation concentration
k , *J/(mol.K)* - Boltzmann constant
K, (-) - proportionality constant

M, *kg/mol* - molecular mass
N_A, *Number/mol* - Avogadro's number
r, *m* - radius of nucleus
t_{ind} , *s* - induction time
V_m, m^3 - molecular volume
ΔG , *J* - excess Gibbs free energy factor

Greek Symbol
γ , *mN/m* - interfacial tension
Superscript
* - saturation
Subscript
S - solid

REFERENCES

1. E. D. Sloan, C. A. Koh, "Clathrate Hydrates of Natural Gases", Taylor & Francis, CRC Press, 2008.
2. J. D. Lee, R. Susilo, and P. Englezos, *Chem. Eng. Sci*. **60**,4203, 2005.
3. H. Ganji, M. Manteghian, K. Sadaghianizadeh, M. R. Omidkhah, H. RahimiMofrad, *Fuel Process.Technol*. **86**, 434, 2007.
4. Y. F. Makogon, *J. Nat. Gas. Sci. Eng*. **2**, 49, 2010.
5. C. Y. Sun, G. J. Chen, *Fluid Phase Equilib*., **242**, 123, 2006.
6. C. F. Ma, G. J. Chen, F. Wang, C. Y. Sun, T. M. Guo, *Fluid Phase Equilib*., **191**, 41, 2001.
7. M. Erik, M. Freer, M. S. Selim, E. D. Sloan, *Fluid Phase Equilib*.p **185**, 65, 2001.
8. M. Clarke, and P. Bishnoi, "Measuring and modeling the rate of decomposition of gas hydrates formed from mixtures of methane and ethane", Chem. Eng. Sci. **56**, 4715, 2001.
9. P. Englezos, N. Kalogerakis, P. D. Dholabhai, P. R. Bishnoi, *Chem. Eng. Sci*.p **42**, 2647, 1987.
10. H.C. Kim, P.R. Bishnoi, R. A. Heidemann, S.S.H. Rizvi, *Chem. Eng. Sci*., **42**, 1645, 1987.
11. H. Luo, C. Sun, Q. Huang, B. Peng, G. Chen, *J. Colloid. Interface. Sci*., **297**, 266, 2006.
12. M. Lin, G.J. Chen, C.Y. Sun, *Chem. Eng. Sci*., **59**, 44, 2004.
13. Z.G. Sun, R.Z. Wang,R S. Ma, "Natural Gas Storage in Hydrates with the Presence of Promoters", Energy. Converse. Manage. **44**, 27, 2003.
14. S. Ghader, M. Manteghian, M. Kokabi, R. Sarraf, *Chem. Eng. Technol*., **30**, 8, 2007.
15. C.Y. Tai, W.C. Chien, *J. Cryst. Growth*, **237**, 2142, 2002.
16. J. W. Mullin, Zacek, *J. Cryst. Growth*, **253**, 515, 2003.
17. J.W. Mullin, "Crystallization" ,Butterworth–Heinemann, Oxford, 2001.
18. P. Tishchenko, C. Hensen, K. Wallmann, C. S. Wong, *Chem. Geology*, **219**, 37, 2005.
19. A. Mersmann *J. Cryst. Growth*, **102**, 841, 1990.
20. P. Bennema, O. Sohnel, *J. Cryst. Growth*, **102**, 547, 1990.